




Article

Structural Controls of Ore Mineralization in a Polydeformed Basement: Field Examples from the Variscan Baccu Locci Shear Zone (SE Sardinia, Italy)

Antonio Funedda ^{1,*}, Stefano Naitza ¹, Cristina Buttau ¹, Fabrizio Cocco ¹ and Andrea Dini ²

¹ Dipartimento di Scienze Chimiche e Geologiche, Università degli Studi di Cagliari, Cittadella Universitaria (Blocco A), S.S. 554 bivio per Sestu, 09042 Monserrato (CA), Italy; snaitza@unica.it (S.N.); cbutttau@gmail.com (C.B.); fabrcocco@gmail.com (F.C.)

² Consiglio Nazionale delle Ricerche (CNR)-Istituto di Geoscienze e Georisorse, 56100 Pisa, Italy; andrea.dini@igg.cnr.it

* Correspondence: afunedda@unica.it

Received: 2 July 2018; Accepted: 11 October 2018; Published: 16 October 2018



Abstract: The Baccu Locci mine area is located in a sector of the Variscan Nappe zone of Sardinia (the Baccu Locci shear zone) that hosts several type of ore deposits mined until the first half of the last century. The orebodies consist of lenses of Zn–Cu sulphides, once interpreted as stratabound, and Qtz–As–Pb sulphide ± gold veins; the implication of structural controls in their origin were previously misinterpreted or not considered. Detailed field mapping, structural analyses, and ore mineralogy allowed for unraveling how different ore parageneses are superimposed each other and to recognize different relationships with the Variscan structures. The sulphide lenses are parallel to the mylonitic foliation, hosted in the hinges of minor order upright antiforms that acted as traps for hydrothermal fluids. The Qtz–As–Pb sulphide veins crosscut the sulphide lenses and are hosted in large dilatational jogs developed in the hanging wall of dextral-reverse faults, whose geometry is influenced by the attitude of reverse limbs of late Variscan folds. The ores in the Baccu Locci shear zone are best interpreted as Variscan orogenic gold-type; veins display mutual crosscutting relationships with mafic dikes dated in the same district at 302 ± 0.2 Ma, a reliable age for the mineralizing events in the area.

Keywords: sulphide lenses; hinge trap; dilatational jogs; orogenic gold; mafic dikes; mineralization chronology; arsenopyrite; late Variscan strike-slip faults

1. Introduction

Structural controls of ore deposits hosted in poly-deformed low-grade metamorphic basements are often not easy to recognize, even more so when there are multiple generations of mineralization, mostly because the relationships between structures and ore bodies are often not clear. The correct understanding of the structural controls is, in fact, relevant for defining the characteristics of the deposit, its emplacement style, its age, and therefore, its origin. In some cases, the difficulties in unravelling the tectonic structures prevent the understanding of the ore bodies' geometry, leading to mistakes in mineral exploration, evaluation of ore deposits, mine planning, and even mineral exploitation. Recognizing whether the structural controls on ore deposits are “passive”, and therefore attributable to tectonic structures developed before mineralization, or, conversely, “active,” i.e., related to tectonic structures progressively evolving with mineralization, can provide valuable indications in this sense. Indeed, passive structural controls imply that there are no direct correlations between tectonic and mineralizing events; the physical parameters that characterized the deformational

events, e.g., thermo-baric conditions, presence of fluids, state of stress, etc., were independent from mineralization processes and they had no influence on ore formation. Conversely, in the case of active controls, these features were critical for mineralization and shaped both the deformational context and the genesis of the ores.

In the nappe zone of the Variscan basement of SE Sardinia, several Sb–W, As–Au, and As–Pb–(Cu, Zn, Ag, Au) ore deposits are located along a lower green-schist facies mylonitic belt, folded by a plurikilometric antiform (the Flumendosa Antiform) during the Variscan collisional phases and then affected by extensional tectonics. During the postcollisional extension, early phases were characterized by ductile-type structures that, with progressive exhumation of deeper tectonic units, further evolved in brittle–ductile to brittle regimes [1], supporting large-scale hydrothermal fluid circulation in the crust. In this frame, mineralization processes and ore deposition were structurally controlled, both passively and actively, at all scales.

In this work, we present a case study of the mineralized systems occurring in the Baccu Locci mine area, located in the core of the Flumendosa Antiform. In this area, several stacked tectonic units are separated by thick mylonitic zones and folded together [2]. Exhumation of the antiformal core is evidenced by the superposition of brittle–ductile and brittle structures over ductile ones; accordingly, different kinds of structurally controlled mineral deposits exposed in the area allow a distinction between passive and active emplacement styles, also leading to a relative chronology of tectonic and mineralizing events. Recent studies in the Baccu Locci mine area [1,3–5] highlighted that: (1) ore formation was structurally controlled and related to the tectonic evolution, during late Variscan extensional phases, of the Baccu Locci regional shear zone, and (2) the relationships between different ores materialize a superposition of tectonic events, further complicated by mafic magmatism and diking. Apart from this general picture, however, several unsolved issues still persist: (1) type and timing of different mineralization, (2) their relationships with tectonic structures and structural controls, (3) ore mineral associations and mafic dikes, and (4) relationships with regional and local stress fields.

In this paper, we intend to contribute to the first two issues and provide some new data for the third one.

2. Geological and Ore Deposits Outline of Baccu Locci Mine District

2.1. Regional Geology

The section of Variscan chain exposed in Sardinia consists of three tectono-metamorphic zones: (1) an inner zone in the north, with medium- to high-grade regional metamorphism, thrust on (2) a nappe zone in central-south, with low-grade regional metamorphism, in turn thrust on (3) a foreland zone in the southwest, non-metamorphosed or with very low-grade regional metamorphism (Figure 1a,b). The emplacement of the tectonic units is generally from the top to the south, with some exceptions [6]. At the map scale, in the nappe zone a distinction can be made between external nappes in the south, displaying a well recognizable lithostratigraphic succession, and internal nappes in the central-north, where it is not easy to recognize the litho-stratigraphic succession. The study area is part of the external nappe zone (Figure 2) and it consists of three tectonic units (from the bottom: Riu Gruppa, Gerrei, and Meana Sardo units) stacked one above the other during the Variscan shortening phases and then affected by late orogenic extension (Figure 3).

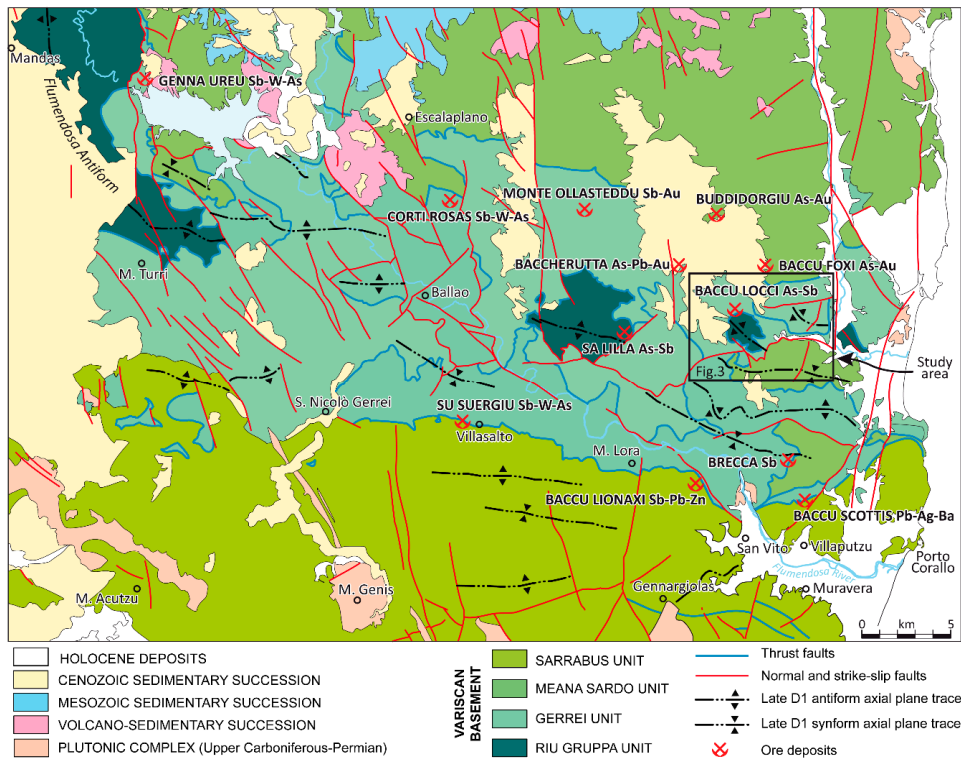
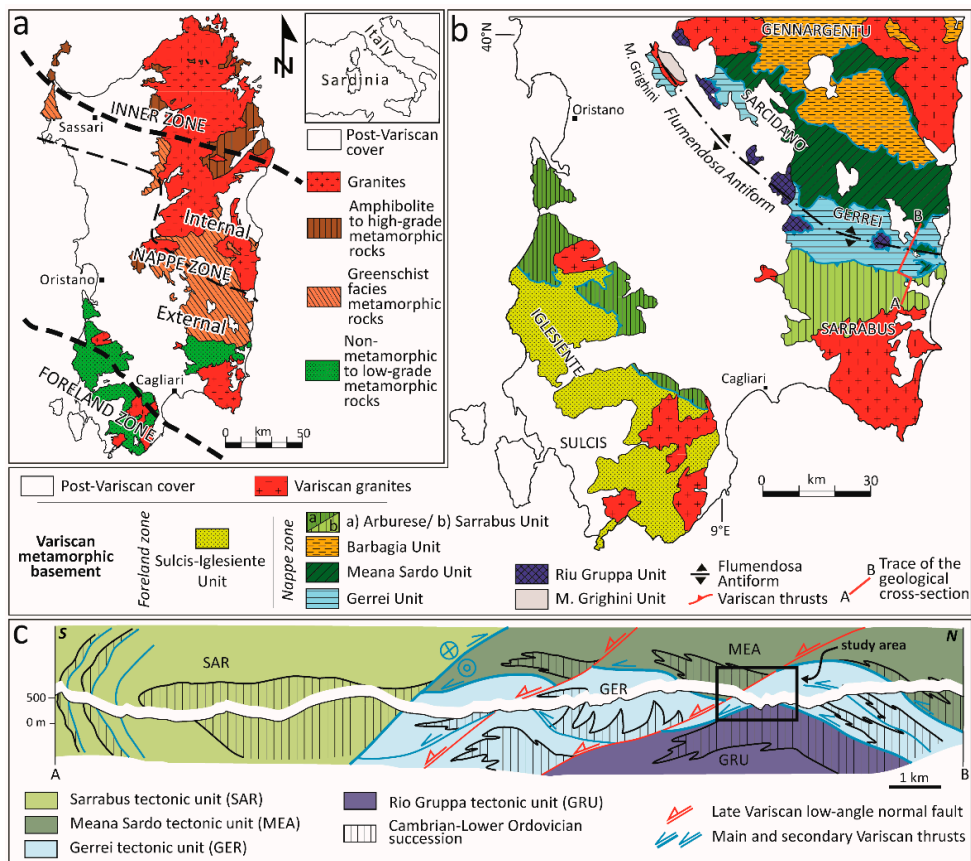


Figure 2. Tectonic sketch map and mineral deposits of the Gerrei district.

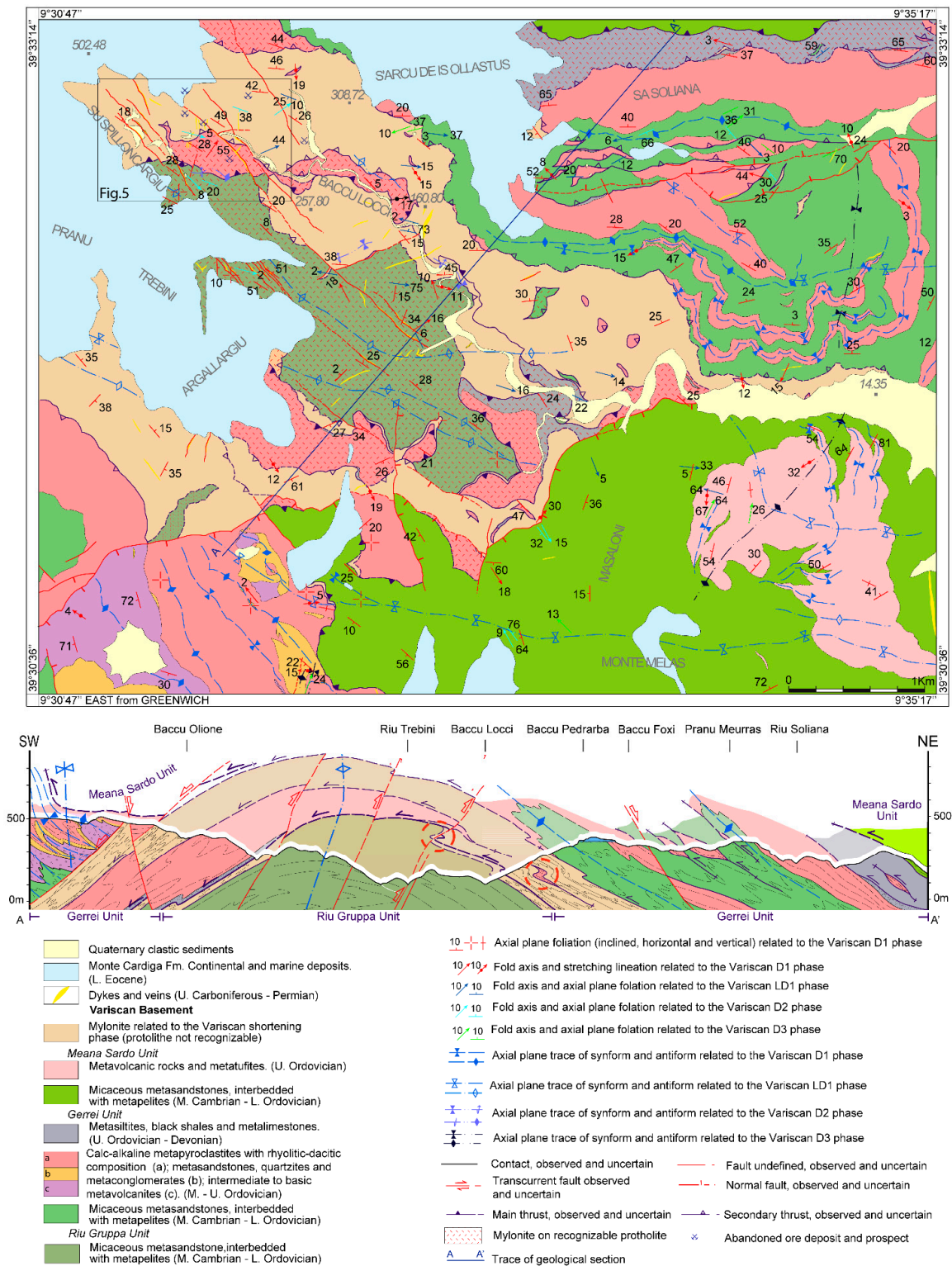


Figure 3. Structural schematic map of the Bacchu Locci shear zone and geological cross-section, after [2]. In the geological cross-section, red circles point out D2 folds that are schematically represented in Figure 15.

2.1.1. Stratigraphic Outline

The tectonic units share a similar lithostratigraphic outline (with some differences, especially in the Middle Ordovician volcanic sequences), which consists of four middle Cambrian to lower Carboniferous successions, separated by three large regional unconformities [8]. They are:

- a mainly siliciclastic succession, with rare interlayered volcanic rocks, of middle Cambrian to Early Ordovician age (*Arenarie di San Vito* Fm.);
- a Middle Ordovician volcano-sedimentary succession with tuffites, metavolcanoclastites, and interlayered epiclastites, andesitic in the lower part (M. S. Vittoria Fm.) and rhyolitic in the upper part ("*Porfiroidi*" Auct. Fm.); the basal contact of this succession is marked by some discontinuous conglomerates (*Metaconglomerato di Muravera* Fm.);
- a siliciclastic to carbonatic succession of Late Ordovician to early Carboniferous age, with lithic sandstones and arkosic arenites (*Metarose di Genna Mesa* Fm., Late Ordovician), siltstones and marls (*Scisti di Rio Canonis* Fm., Late Ordovician.), black shales and limestones ("*Scisti neri a graptoliti*" Auct. Fm., Silurian to Early Devonian; "*Calcari di Villasalto*" Auct. Fm., Early Devonian to early Carboniferous);
- a lower Carboniferous siliciclastic sequence with conglomerates, sandstones, and olistoliths of the older formations that unconformably rests on the Devonian formations, which does not crop out in the study area (*Pala Manna* Fm., early Carboniferous); it is the youngest formation involved by the Variscan orogeny in Sardinia.

The metamorphic basement of SE Sardinia is then intruded by an upper Palaeozoic (upper Carboniferous to lower Permian) intrusive complex. Lower Permian leucogranitic rocks outcrop close to the study area in the Quirra sector [9]; they belong to a calc-alkaline, ferroan, F-bearing, ilmenite-series intrusion, part of a magmatic suite dated at 286 ± 2 Ma [10]. The entire period of granitoid magmatism is associated with calc-alkaline volcanism [11] and with widespread mafic and felsic diking [12]. Early diking phases are represented by swarms of calc-alkaline (spessartitic) mafic dikes; one of them, crosscutting the same tectonic unit in a nearby area, is dated at 302 Ma [13].

The early Eocene *Monte Cardiga* Fm., made up of conglomerates, sandstones, and marls that are deposited in littoral environments lies unconformably on the metamorphic basement and the intrusive complex. In the surrounding areas, the oldest deposits that unconformably cover the Variscan basement are Middle Pennsylvanian continental deposits [14].

2.1.2. Structural Outline

The oldest tectonic features that are recognizable in the Baccu Locci mine district involve the lower Carboniferous rocks and are related to the Variscan orogeny. Indeed, there is no evidence of the pre-Middle Ordovician tectonic structures recognized in adjacent areas [7], as they were probably obliterated by Variscan deformation. The overlap of several early to late Carboniferous deformation events is evidence that a D1 collisional phase with crustal thickening and subhorizontal shortening occurred under ductile conditions and a D2 postcollisional extension with the reactivation of some of D1 structures occurred in the ductile–brittle transition (Figure 4) [6,8,15]. The D1 phase is characterized by a general SSW-directed nappe emplacement, regional folding and thrusting, and syntectonic regional lower green-schist facies metamorphism. An exception is represented by the Sarrabus unit, the shallowest nappe of the stack, which crops out south of the study area and it is emplaced from the top to the west [16]. The D1 early shortening structures are large kilometer-scale recumbent isoclinal folds facing southward, with well-developed penetrative axial plane foliation—generally a slaty cleavage produced in lower green-schist facies metamorphism—followed by almost contemporary south-southwest thrusts that produced thick mylonitic belts. Development of such shear zones between the different tectonic units, thick up to several hundred meters, is common in the Variscan basement of Sardinia [17–24]. Among them, the Baccu Locci shear zone is one of the most noteworthy [3]. It can be followed in the field for more than 30 km; the study area is located on its eastern side. The Baccu

Locci shear zone is characterized by widespread and penetrative mylonitic foliation with a mineral assemblage typical of lower green-schist facies metamorphism that is parallel to the large thrust and generally cuts at a low angle the early D1 axial plane foliation [3]. The deformation is highly partitioned; in the core of the shear zone, it is not possible to recognize the mylonite protolith, although several slices of less deformed rocks have been recognized and mapped [2,3,19]. (Note that, following the choice by [2,3], in Figures 3 and 5 we distinguished the mylonite whose protolith is not recognizable from the mylonite whose protolith is still recognizable). At a later stage during the collisional phase, a late-D1 (LD1) N-S shortening event led to development at a regional scale of large, weakly east-plunging upright folds, with axes up to 50 km long that refolded both isoclinal folds and ductile shear zones. Of these late folds, the main fold is the Flumendosa Antiform [1] (Figures 1 and 2), which runs roughly from WNW to ESE for more than 50 km, folding the D1 nappe stack. In detail, the Flumendosa Antiform consists of some minor order antiforms and synforms with km-size wavelength. One such northern minor order folds crops out in the study area. The LD1 axis is generally east-plunging, and at the hinge zone, a subvertical spaced crenulation cleavage discontinuously developed. Then, the LD1 folds were in turn deformed during the D2 postcollisional extensional phase. The limbs of the LD1 antiforms are deformed by several asymmetric recumbent folds with subhorizontal axial planes and axes parallel to the LD1 limb attitude [1] (Figure 4). The D2 folds are overturned away from the antiformal hinge zone [1]. They are often associated with low-angle normal shear zones that allowed for the exhumation of deeper units and enhanced the antiformal structure. They have opposite structural-facing direction in the fold flanks: north-facing in the northern limb and south-facing in the southern limb. Their major order wavelength exposed in the field is about 30 to 40 m. Folds with “outer” structural facing and low-angle normal faults are interpreted as produced by vertical shortening of steeply inclined bedding and earlier foliations. During exhumation, rocks were progressively carried to shallower structural levels, where brittle behavior became prevalent. Thus, the deformation style changed, and the final stage of postcollisional extension was accommodated by high-angle normal faults [6]. A D3 folding event, with vertical axial planes and axis trend changing from N-S to N 40°, is also recognized, but it is still not clear whether it could be related to a final stage of postcollisional extension or to the following D4 strike slip faulting [8]. Finally, D4 strike-slip faults affected the exhumed basement but did not involve the Permian to Eocene successions that crop out in the study area. At the Variscan Realm scale, a late strike-slip tectonics is from far recognized. Moreover, is clearly observable in the field that the lower Permian granitoids postdate the D1, D2, and D3 structures, whereas there is less evidence about their relationship with strike-slip tectonics. As we will describe below, LD1 and D2 folds, as well as late faults, played a significant role in controlling the geometry of orebodies.

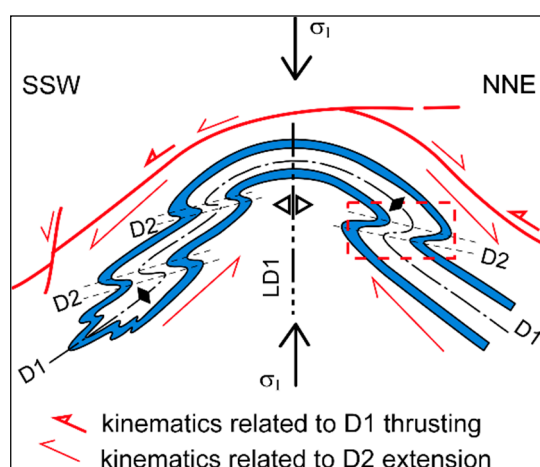


Figure 4. Schematic relationships between D1, LD1, and D2 structure. Note the development of recumbent D2 folds in the limb of upright LD1 antiform (modified after [1]). The red dashed box indicates the location of the scheme in Figure 15.

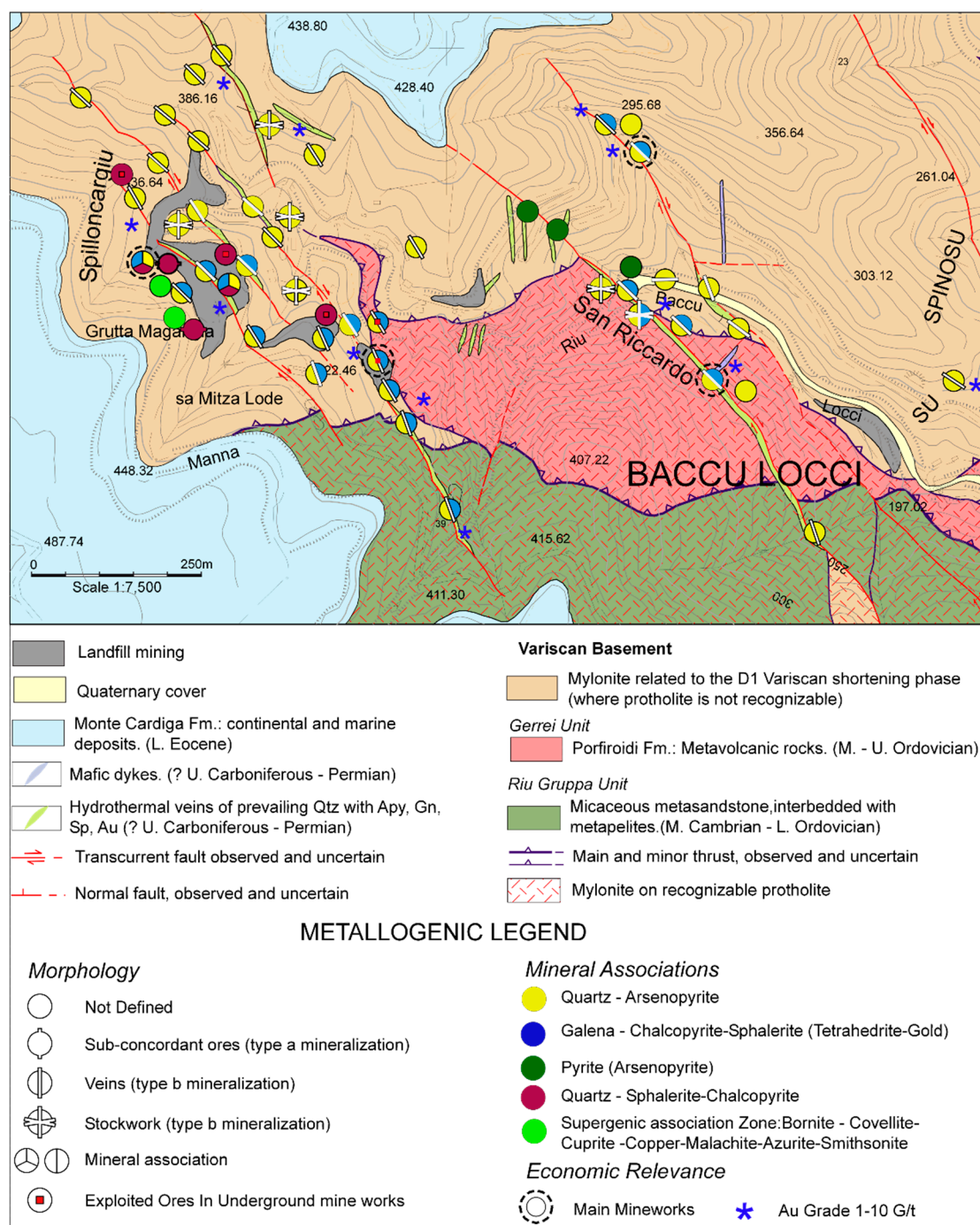


Figure 5. Mineralized outcrops in the Baccu Locci mine area, after [2].

2.2. The Gerrei-Sarrabus Metallogenic District

The Gerrei-Sarrabus region has been historically the second most important mining area in Sardinia and the most important antimony district in Italy (Villasalto–Ballao district). Several reviews of the district’s mineral deposits have been done in the past [25–27], including a recent attempt to interpret some of the main mineral associations in the Variscan metallogenic epoch of Sardinia [28]. The main mineral deposits of the region include the following (Figure 2):

- (a) Zn–Cu–Pb sulphide lenses, disseminations, and ores;
- (b) Sb–W, As–Au, and As–Pb–(Cu, Zn, Ag, Au) mesothermal systems with quartz–sulphide veins, stockwork, and disseminated ores;

- (c) Mo–W–F greisen and vein-type ores;
- (d) F–Ba ± Pb–Ag–Cu–Zn vein systems.

Ores of (a) and (b)-types are hosted in the Palaeozoic metamorphic basement, and mostly occur in the northern part of the district (Gerrei); (c) type ores are hosted in and/or related to the suite of F-bearing Permian granites of San Vito and Quirra intrusions [9,29]; and, (d) type ores occur prevalently in the southern part of the district (Sarrabus), are broadly typified by the “Sarrabus Silver Lode” [30] and Silius [31] deposits, and they are possibly related to another suite of F-rich Permian granites (Sette Fratelli and Monte Genis intrusions [9]). Although still very lacking and non-systematic, some isotope and fluid inclusion data on different Gerrei-Sarrabus ore deposits are available from several recent studies [10,25,30–32].

Only (a) and (b) type ores are present in the study area, and thus will be considered in detail in this work. Both types are structurally controlled and are located at different structural levels.

3. Materials and Methods

To reconstruct the orebodies and their relationships with the tectonic structures, detailed field work was performed, mapping at 1:5000 and 1:10,000 scale both mineral deposits and tectonic features (foliations, folds, faults, kinematic indicators). The surface data have been integrated with the subsurface data, in rare cases directly sampled in the mine when still accessible, but generally taken from 1:500 scale exploitation maps related to the last period of mining activities in 1961. The grade of detail reported in those maps allows us, in some cases, to recognize not only the mine works, but also the geometries of the ores. Importing and processing these data in the three-dimensional (3D) workspace of Rhinoceros© and Move (©Midland Valley, Edinburgh, Scotland, UK), allow minimization of the unbalanced area and validation of the geological-structural map (see description in [2]).

The kinematic analysis of fault slip data was performed using FaultKin 5.2 by Allmendinger [33]. The slip direction and the sense of slip were inferred from several types of kinematic indicators—slickenlines, tension gashes, drag folds, and S-C structures—all collected along the D4 transpressive faults and related orebodies. They all indicate similar kinematics, suggesting that the paleostress remained the same during vein formation. The occurrence of different types of kinematics indicators during the same tectonic event (i.e., D4 faulting), sometimes exactly along the same fault, can depend on the mechanic behavior of the involved rocks. In general, when the damage zone is large enough and there is a relevant grain-size reduction in cataclased rocks, S-C-like fabric easily developed, although physical condition and deformation mechanisms are those typical of shallow structural levels [34,35]. The orientation of the principal strain axes that was achieved from fault slip data analysis gives an idea about the paleostress field accounting for the fault kinematics.

In this study, ore mineralogy and microtextural studies were performed on polished sections by optical microscopy in reflected light. Several transmitted light studies on thin sections of ores and their host rocks have been performed in past works [3,5,7,19].

4. Results

4.1. Structures and Mineralization in the Baccu Locci Mine Area

The mineralized deposits of the Baccu Locci mine area (NE Gerrei, Figures 2 and 5) occur in a key area for studying the structural and metallogenic evolution of the region. In Baccu Locci, the ores are exposed at different structural levels along the hinge zone of the Flumendosa Antiform, hosted by the strongly mylonitized siliciclastic metasediments and felsic metavolcanics of the Gerrei tectonic unit [3]. Both Zn–Cu–Pb sulphide lenses (*type a* mineralization) and Qtz–As–Pb sulphide hydrothermal vein deposits (*type b* mineralization) are represented in the area, where it is also possible to recognize spatial relationships of ore deposits with coeval mafic dikes [4].

4.1.1. The Zn–Cu–Pb Sulphide Lenses (*Type a* Mineralization)

Zn–Cu–Pb sulphide lenses occur in the Su Spilloncargiu mine sector (Figure 5), hosted in phyllitic quartz–mylonite rocks (Figure 6a–e), whose protolith was made mainly by siliciclastic sediments, with a high occurrence of recrystallized quartz and muscovite, metamorphosed in lower green-schist facies during the Variscan Orogeny. Due to supergene alteration (Figure 7b), the Spilloncargiu primary ore is not well exposed on the surface; access to underground works is not easy, but some samples can be found in the dumps of the lowermost mineworks.

Ore Mineralogy and Textures

At the outcrop scale, the mineralization shows a laminated texture, with the sulphides being disposed along the mylonitic foliation. At the microscopic scale, it is possible to recognize that the deposition of ore minerals is polyphasic. The first event is characterized by dark ferroan sphalerite with abundant and finely dispersed chalcopyrite and pyrrhotite inclusions (*chalcopyrite disease* [36]). This early sphalerite is the prevailing sulphide in the ore (Figure 7a) and it displays an evident cataclastic texture. Voids and fractures in cataclased sphalerite aggregates are filled by abundant galena, chalcopyrite, and pyrite, while arsenopyrite and tetrahedrite-group minerals are usually subordinate (Figure 7b). Galena crystals show only slight evidence of deformation and have not suffered the cataclastic deformation that involved the sphalerite. Gangue minerals are subordinate to sulphides and consist of two recognized generations of gray quartz: early quartz, macrocrystalline, and cataclased, is related to the sphalerite stage of mineralization; late quartz is microcrystalline, fills the microfractures, and is associated with galena and other sulphides (Figure 7c). Wall rock hydrothermal alteration is difficult to recognize, due to late superposed supergene phenomena, but it certainly included silicification and pervasive dispersion of carbonaceous matter, possibly precipitated during mineralization, which gave the sulphide-bearing mylonite a distinctive black color. No free gold was ever identified in this ore, whose Au geochemical contents are very low [2,26,37].

Structures

The old mine exploited several lenticular sulphide orebodies that were located in the hinge zone of a km-size open, upright antiform (a minor order structure of the largest Flumendosa Antiform) related to the LD1 collisional phase (see cross-section in Figure 3 and the scheme in Figure 4). The antiform axis weakly plunges toward N120 (Figures 3 and 8); the structure deformed the foliated isoclinal folds related to the early stage of shortening (D1 Variscan phase) and the mylonitic shear zone that separates the Riu Gruppa and Gerrei tectonic units. The exploited sulphide lens-shaped orebodies developed parallel to the D1 mylonitic foliation, which in this area is at a low angle with the D1 axial plane foliation (Figure 9). There is no evidence of the primary bedding, completely transposed during the D1 tectonic phase. The lenses attain a maximum thickness of 6–7 m for maximum extension in a strike of 80–100 m. Although located in the hinge zone of an antiform, they cannot simply be classified as typical saddle reefs, as they do not display the classical triangular shape related to hinge collapse. The main dip of the mineralized lenses is up to 20° toward N 140°, so more or less in the axis plunge direction. The shape of the orebodies is well detectable by studying the old room-and-pillar mineworks, still being partially accessible.

In detail, it is possible to recognize crosscut relationships between different events of mineralization. The large lens-shaped orebodies are mainly characterized by abundant Zn–Cu sulphides forming veinlets 1 to 10 cm in size hosted in the mylonite (Figure 6a), being generally parallel to the mylonitic foliation of the hinge zone (Figure 9). Galena, chalcopyrite, pyrite, and other sulphides are arranged in cm-sized veinlets that involve the hosting rocks for about 1 m of thickness; they cut at low angle the Zn–Cu lenses (Figure 6e), thus postdating them. In the field, these veins became progressively steeper and more arsenopyrite-rich (Figure 7c).

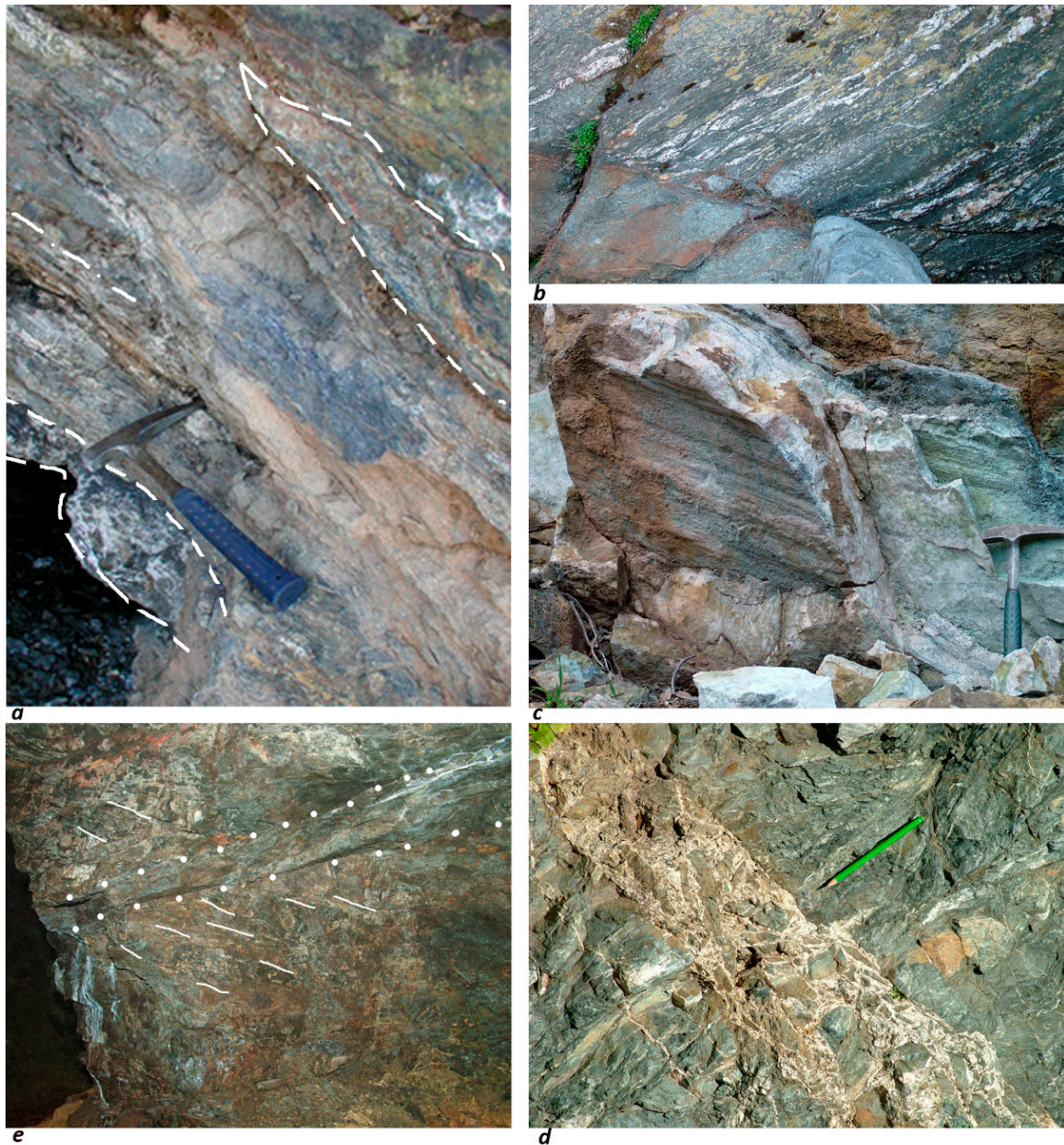


Figure 6. Outcrop pictures of the Bacchu Locci mineral deposits: (a) Su Spilloncargiu mineworks: Zn–Cu–Pb sulphide lens ore (*type a* mineralization). The thin sulphide “beds” (dashed line) are parallel to the Variscan mylonitic foliation (solid line). (b) Bacchu Trebini outcrop (*type b* mineralization): Qtz–As–Pb sulphide sheeted veins along a SW-dipping brittle shear zone. (c) Along Rio Bacchu Locci, close to San Riccardo mineworks (*type b* mineralization): Qtz–As–Pb dm-size vein with subhorizontal slickenlines. (d) Bacchu Trebini outcrop (*type b* mineralization): Fault breccia with Qtz–As–Pb sulphides wrapping wall rock clasts along SW-dipping fault. (e) Su Spilloncargiu mineworks (*type a* mineralization): in a pillar of the exploited mine a *type b* Qtz–As–Pb sulphide vein (white dotted line) crosscuts a sulphide lens that is parallel to Variscan foliation (white lines).

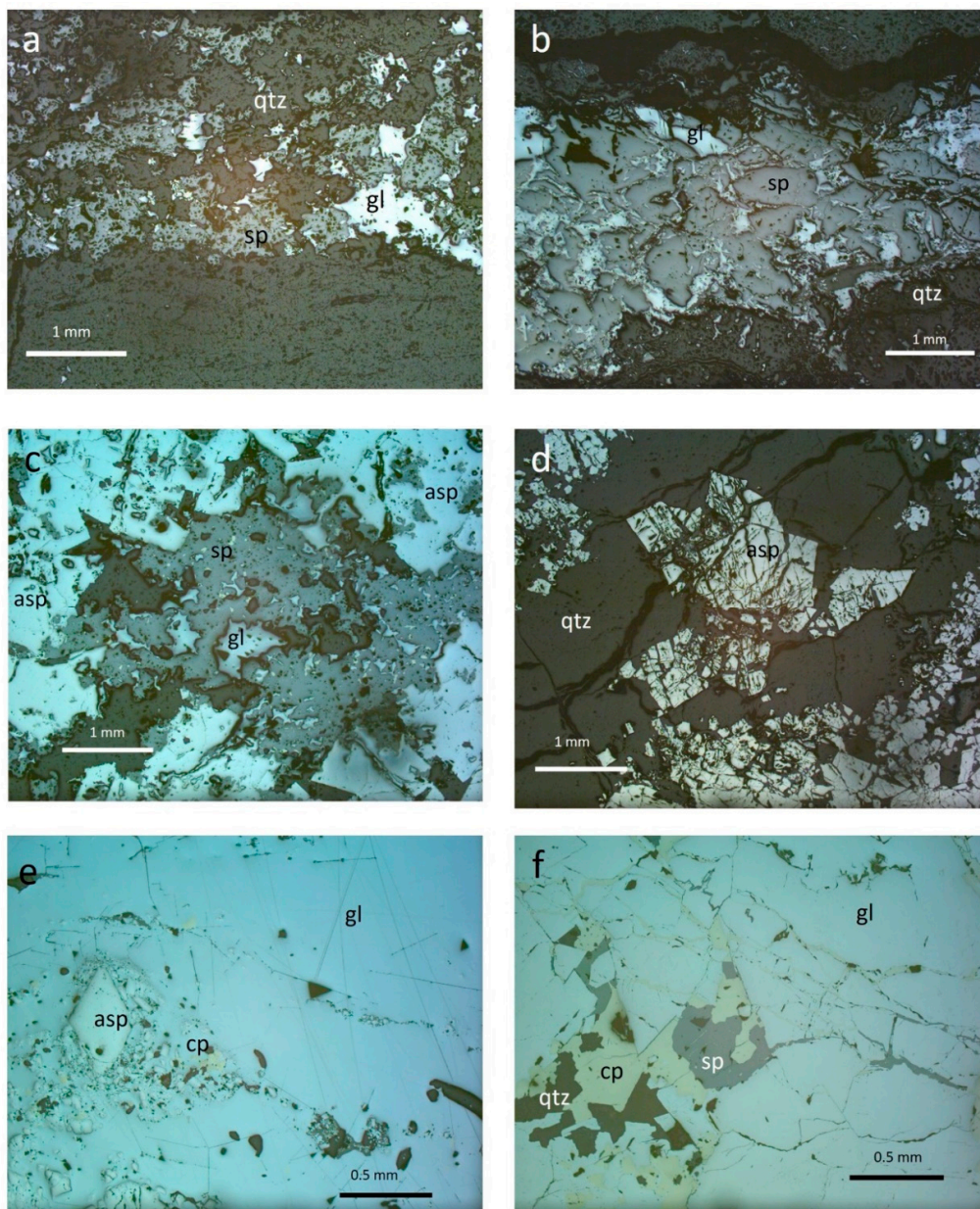


Figure 7. Microtextural features of ores in the study area (polished sections, reflected light): (a) Su Spilloncargiu mineworks, early mixed sulphide ore (*type a* mineralization): Brecciated quartz–sphalerite layer infilled by late galena; the mineralized layer follows the S_m foliation and exhibits sharp contact with a phyllosilicate layer in the mylonitic matrix; high-Fe sphalerite shows a distinct *chalcopyrite disease* with large chalcopyrite and pyrrhotite exsolutions. (b) Su Spilloncargiu mineworks, early mixed sulphide ore (*type a* mineralization cementation zone): Brecciation of sphalerite, infilled by primary galena, is particularly highlighted by cementing fine veinlets of secondary galena. (c) Su Spilloncargiu mineworks, quartz–arsenopyrite veins (*type b* mineralization crosscutting *type a* mineralization): Arsenopyrite aggregates enveloping early sphalerite aggregates (with some galena) from mixed sulphide ore. (d) Su Spilloncargiu mineworks, quartz–arsenopyrite veins (*type b* mineralization): Typical brecciated arsenopyrite texture, with large aggregates of fractured sub-idiomorphic crystals. (e) San Riccardo mineworks (*type b* mineralization): large galena (chalcopyrite) enveloping arsenopyrite crystals. (f) San Riccardo mineworks (*type b* mineralization): Detail of the late ore, with abundant fractured galena infilled by late chalcopyrite and inclusion poor sphalerite; sphalerite only displays very fine chalcopyrite exsolutions along crystallographic planes. Qtz, quartz, gl, galena, sp, sphalerite, asp, arsenopyrite.

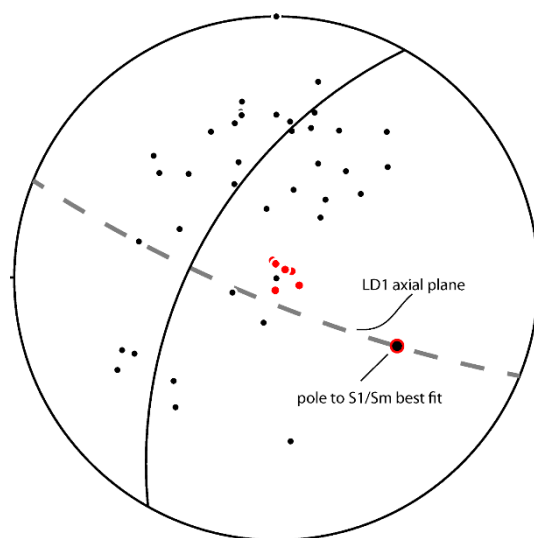


Figure 8. Stereographic projection (equal area, lower hemisphere) of D1 tectonic foliation (black dot), LD1 axial surface (dashed line), and calculated axis (red circle), attitude of sulphide orebodies (red dot).

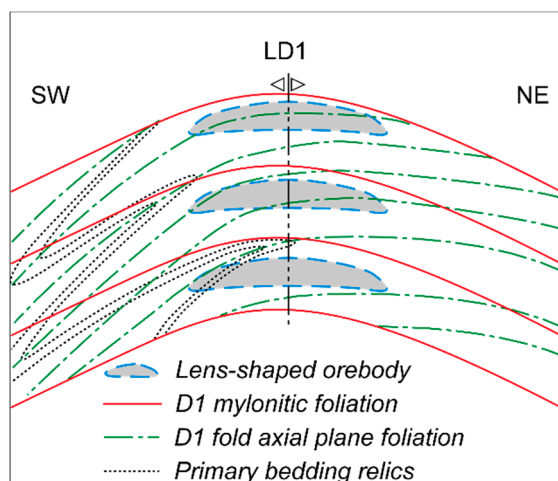


Figure 9. Schematic relationships between lens-shaped sulphide orebodies, D1 fold axial plane foliation, and D1 mylonitic foliation in the hinge zone of LD1 antiform at Spilloncargiu mine works (not to scale).

4.1.2. Qtz–As–Pb Sulphide Vein Systems (*Type b* Mineralization)

Swarms of quartz–As–Pb (Zn, Cu, Ag, Au) sulphide hydrothermal veins occur frequently in the Baccu Locci mine area and in several nearby localities along the highly mineralized Baccu Locci shear zone. The best exposition occurs in the San Riccardo/Su Spinosu mine (Figure 5), where the veins reach the maximum mapped thickness.

Ore Mineralogy and Textures

Textural and mineralogical observations of the Qtz–As–Pb sulphide vein ores are the basis for a general paragenetic sequence that includes: (1) a *pre-ore stage*, with large precipitation of coarse-grained white quartz and rare scheelite [37]; (2) an *As–Fe sulphide stage*, following the diffuse cataclasis of white quartz, with abundant arsenopyrite (I) and pyrite in quartz macro- and microfractures, after an initial arsenopyrite–pyrite dissemination in the wall rock; (3) a *sulphide/sulfosalts stage*, after new cataclasis (Figure 7), with infilling of gray microcrystalline quartz, Pb–Zn–Cu–Ag sulphides (galena, sphalerite, chalcopyrite, argentite), euhedral arsenopyrite (II), phyrrothite, Cu–Ag–Sb–As sulfosalts (tetrahedrite–freibergite, bournonite, stephanite), rare stibnite, and gold/electrum [37,38];

and, (4) a late stage, with cryptocrystalline quartz and pyrite. In the sulphide/sulfosalts stage, textural evidence indicates an initial deposition of galena, which is the most abundant mineral (Figure 7); sphalerite, chalcopyrite, and other sulphides followed. Fine disseminations of euhedral (sometimes needle-shaped) arsenopyrite (II) in cataclased wall rocks are probably related to this stage. Sphalerite in *type b* ores is distinctly different from that in *type a* sulphide lenses, being much less abundant, less deformed, less dark (it shows more evident internal reflections), and much less affected by *chalcopyrite disease*. Wall rock alteration occurred from the earliest stages, but it is substantially limited to narrow zones close to the veins, commonly marked by intense sericitization, sulphidation (fine pyrite dispersion), and silicification; in many outcrops, the footwall of the veins is strongly cataclastic and displays a characteristic black color (*black cataclasite*), further indication of diffuse precipitation of carbonaceous matter during some of the mineralizing phases. A system of E-W quartz–feldspar cm-thick veinlets has been locally observed; it distinctly crosscuts the quartz–sulphide veins and may be related to a different (and very late) phase of fluid circulation in the area. Gold grades in sulphide veins are 1–12 g/t [27,38], with good persistence in the whole mineralized vein system; silver grades are 1000–1200 g/t [27]. The Au/Ag ratio in gold grains is <1, in opposition to regional trends [37]. According to Bakos et al. [37], 10 µm sized gold grains are particularly associated with chalcopyrite and galena/bournonite myrmekitic intergrowths that infill microfractures in cataclased arsenopyrite aggregates.

Structures

Qtz–As–Pb sulphide veins are generally hosted in narrow brittle shear zones, usually not thicker than 10 m, of high-angle faults dipping about 70° toward N 230°, confirming the structural trend recognizable at the scale of the entire district for *type b* mineralization [26,27]. The faults generally involve both the quartz mylonite, whose protolith is not possible to ascribe to one of the mapped formations, and the Ordovician rhyolitic volcanites with augen-textures (“Porfiroidi” Fm.) that constitute some hectometer-sized tectonic slices inside the shear zone (Figure 3).

The faults clearly cut all the ductile D1, LD1, D2, and D3 structures (shear zone, folds, and foliations) and are sealed by the lower Eocene sediments. From the structural map (Figure 3), it is evident that the mineralized faults are parallel to the LD1 antiform axis and are mainly located in the hinge zone. We can interpret this occurrence considering two likely types of reactivation of previous structures, both occurring at a shallower structural level than the LD1 phase. They could be hinge-parallel fractures developed in the fold outer arc, parallel to the *bc* plane according the fold-related joints classification by Hancock [39]; or, more probably, the faults reactivated the noncontinuous, spaced crenulation cleavage that discontinuously developed just in the hinge zone of LD1 antiforms.

The mineralized bodies are lenticular, elongated to laminated veins that are typical of a fault-fill vein system. They can vary from isolated veinlets no more than 1 cm thick to sheeted veinlets and laminated veins in which the hydrothermal mineral component prevails over the host rock component (Figure 6b). Along the fault zones hosting the veins, several kinematic indicators are found, frequently at the contact between veins and wall rocks. In some damage zones there are fault breccia with wall rock clasts wrapped by dominant hydrothermal quartz (Figure 6d); furthermore, some shear zone is characterized by a foliated black cataclasite showing S-C type fabric. Slickensides and striated surfaces occur also on the contact between the fault-fill veins (Figure 6c). Slickenlines, tension gashes and S-C type complex foliations collected along the SW-dipping faults hosting the main quartz–sulphide veins all indicate a dextral strike-slip kinematic with a small reverse component (a tectonic transport direction from the top to the NW, some data are plotted in Figure 10b). A kinematic analysis was performed also considering faults hosting Qtz–As–Pb sulphide veins but with a different orientation allow for us to reconstruct a strain ellipsoid with a subvertical intermediate axis (λ_2 , and subhorizontal shortest (λ_3) and longest (λ_1) axes, respectively, oriented roughly N-S and E-W (Figure 10). Although parallelism between strain and stress ellipsoid cannot be demonstrated and we did not perform a

paleostress inversion, the kinematics suggests a paleostress field with a subhorizontal σ_1 in agreement with strike-slip tectonics.

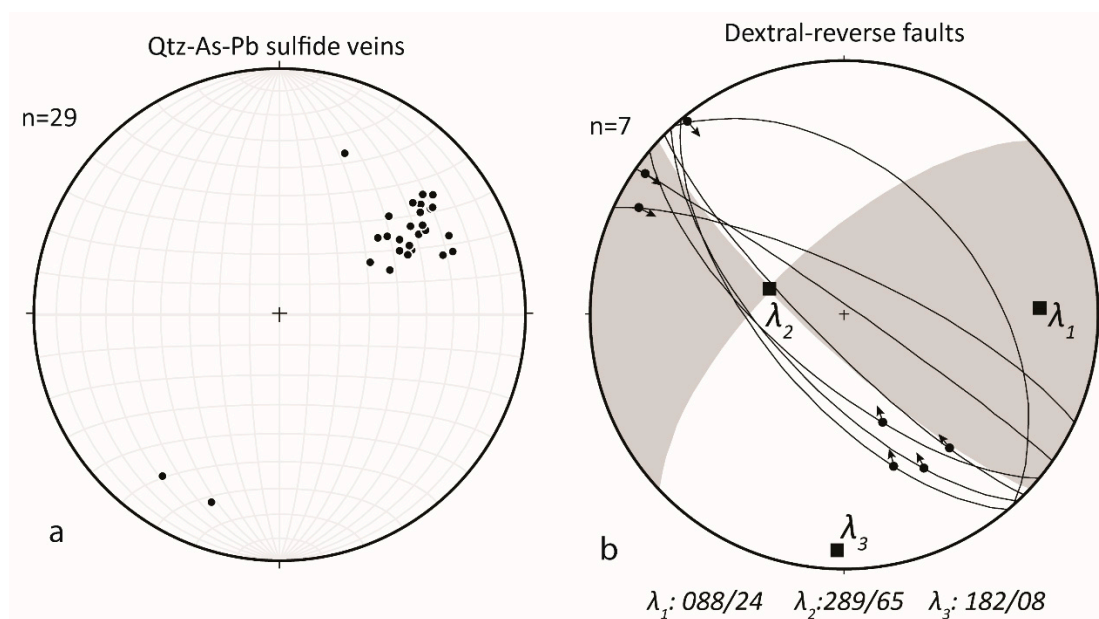


Figure 10. (a) Stereographic projection (equal area, lower hemisphere) of poles to Qtz–As–sulphide main orebodies in the Baccu Locci zone; (b) Kinematic analysis of the SW dipping faults hosting quartz Qtz–As–sulphide veins. λ_1 , λ_2 , and λ_3 are the directions of maximum, intermediate, and minimum strain ellipsoid axes, respectively.

Typical economic orebodies exploited in the past mine were sulphide-rich ore shoots up to 8–9 m thick, extending along the SW-dipping faults 100–300 m along strike, and over 100 m down dip. By using the available detailed maps of mineworks, it is possible to construct a 3D model of these orebodies, particularly for the San Riccardo/Su Spinosu mine (Figure 11b). Along the stretched mineralized zones, the orebody thickness increases where the fault surface is less inclined, almost subhorizontal, and decreases where the fault is steeper, generally becoming no thicker than 2 m. At the underground level 214.68 in the San Riccardo mineworks, which is unfortunately hardly accessible today, this geometry has been observed exactly along section C–C' in Figure 11a, where the fault plane and the sulphide veins are subhorizontal (Figure 12). Although no longer accessible, from the 3D model and from the old mine reports, the room-and-pillar exploitation between levels 201.68 and 179.68 can be considered as a less inclined sector of the fault, marked by an increase in thickness of the orebody (section A–A' in Figure 11a). From these observations, the more relevant economic orebodies of *type b* mineralization may be associated with very large dilational jogs developed on the hanging wall of the transpressive faults (Figure 11a), where the occurrence of less inclined segments connecting the subvertical ones (Figure 11c) produced room for the emplacement of the orebodies during the fault activity.

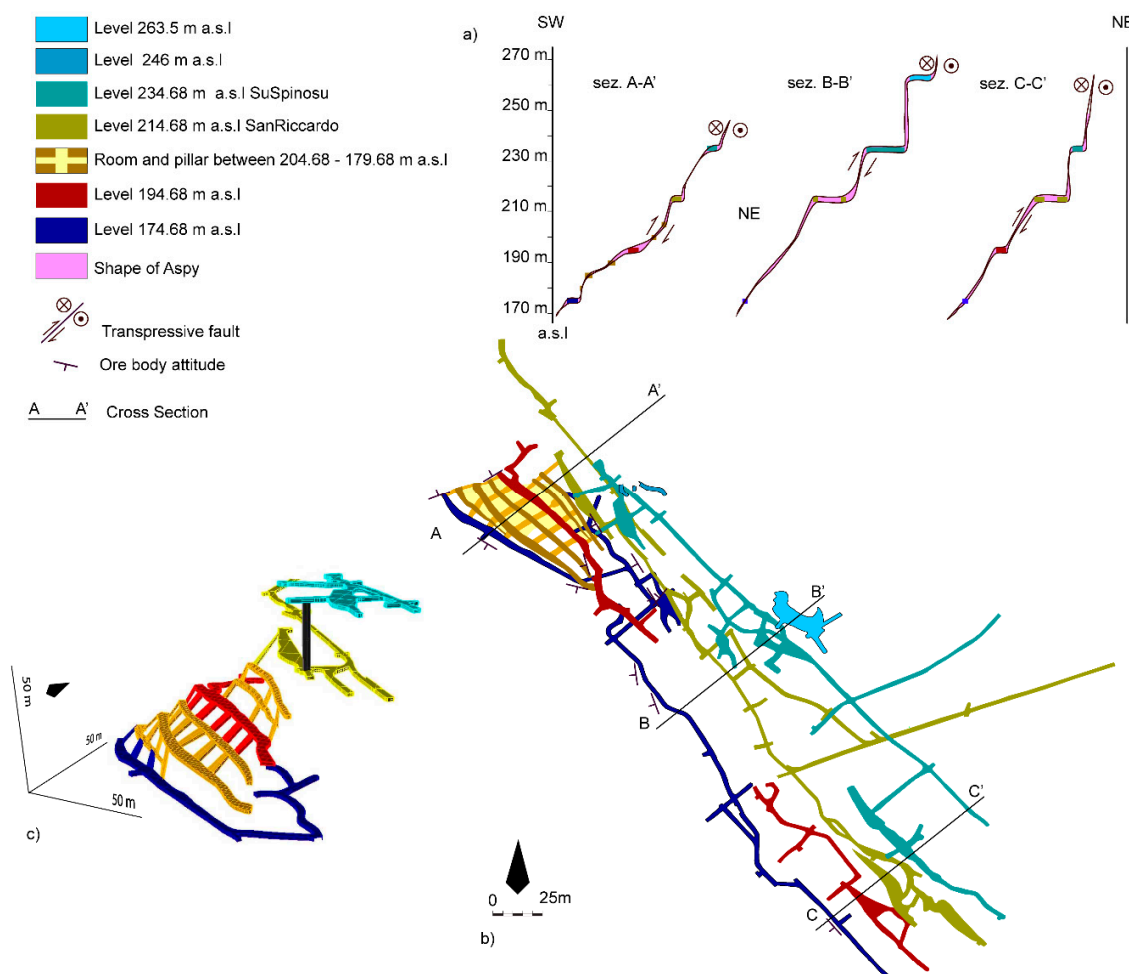


Figure 11. The Baccu Locci/San Riccardo mine, *type b* mineralization (numbers are elevation above sea level, a.s.l.): (a) schematic vertical sections that point out the sigmoid shape of the sulphide veins of the San Riccardo orebodies (see trace in b), interpreted as large dilational jogs; (b) minework plans based on the original mine maps (different levels are identified by colors; and, (c) three-dimensional (3D) model of the northern part of mineworks in b, in the area of section A-A'; note that the orientation is different from the map in b.

4.1.3. Mafic Dikes

Detailed mapping of the Baccu Locci mine area [2] revealed a wide occurrence of mafic dikes, verifying complex mutual geometrical relationships among them and the ores (see also [26,38]). Dikes are variable in size (0.1–10 m thick) and orientation (from subvertical to subhorizontal), with a prevalence of N-S direction. They distinctly crosscut the foliation of the hosting mylonites, extending along for tens of meters. In different outcrops there is clear evidence that the dikes cut across and partly follow the structural pattern of the quartz–sulphide veins. Moreover, they are also locally crosscut by *type b* quartz–sulphide veins. Of particular interest is the relationships along the large dilational jogs that were observed at the San Riccardo mineworks; there, a mafic dike abruptly changes its attitude from subvertical to subhorizontal, following the tectonic foliation in the reverse limb of a D2 recumbent fold, and becoming parallel to the fault plane hosting the *type b* veins (Figure 12a).

Zucchetti [38] first classified the mafic rocks as spessartitic lamprophyres: under the microscope they show an aphanitic to porphyritic (doleritic) texture, with small labradoritic–bytownitic plagioclase, idiomorphic hornblende phenocrysts, and corroded quartz xenocrysts in a strongly altered groundmass; accessory phases are apatite, titanite, magnetite, ilmenite. These features allow for us to frame them among the calc-alkaline mafic dikes widely intruded in the SE Sardinia basement

during the late Variscan extension [12] and recently dated, in the Gerrei district, at 302 ± 0.2 Ma (U–Pb dating on zircon [13]).

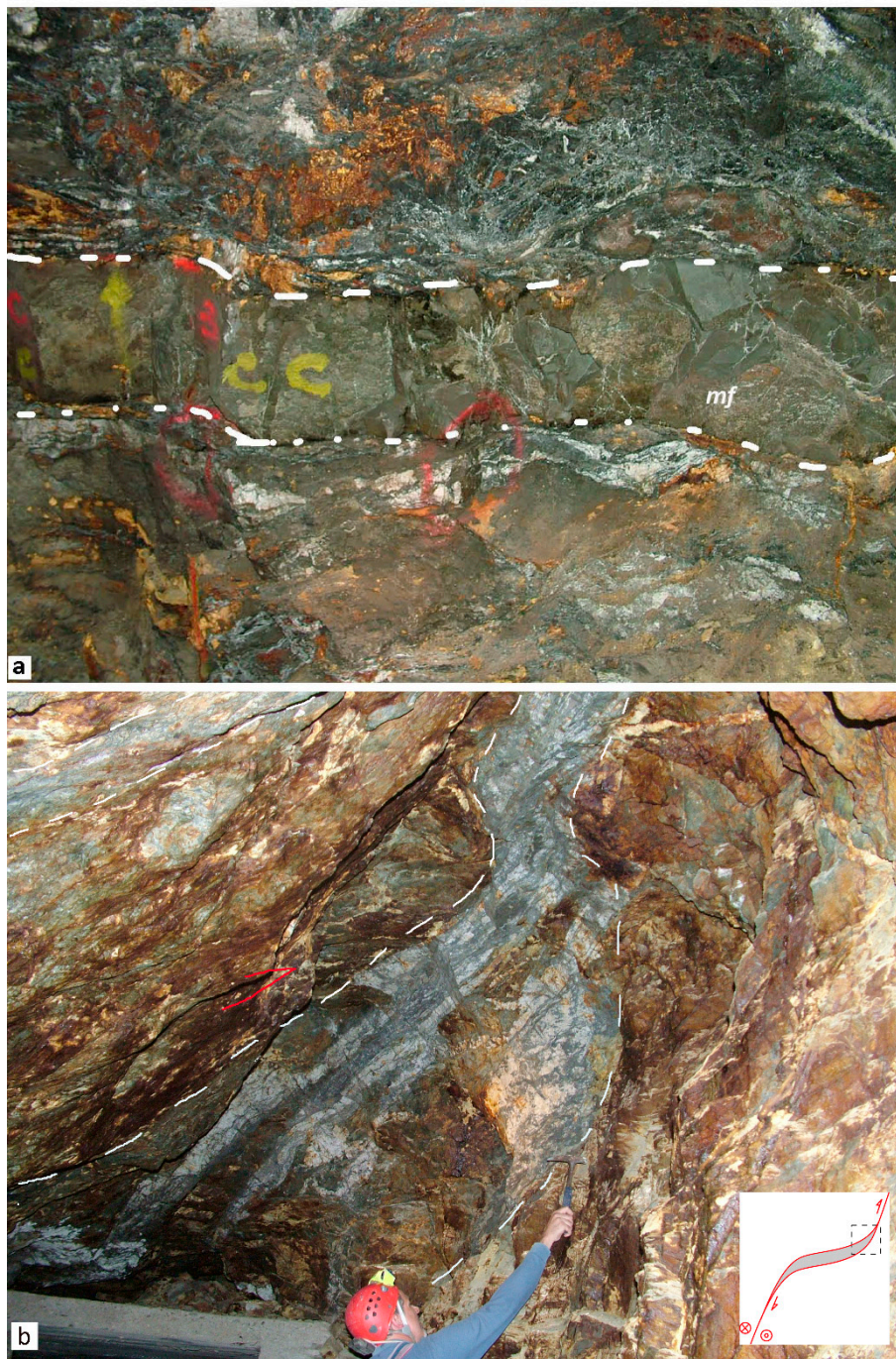


Figure 12. Outcrop relationships between Late Variscan mafic dikes and *type b* ores in the southern branch of San Riccardo underground mineworks: (a) sub-horizontal Qtz–As–Pb sulphides veins parallel to a mafic dike (mf) about 1.0 m thick (contact is highlighted by dashed white line); and, (b) Qtz–As–Pb sulphide ore (underlined by dashed white line) that progressively became less steep toward the left (ESE). The dashed box in the small picture indicates the location of the outcrop respect to the whole lens-shaped orebody. Photo in a is about 2 m to the left (i.e., west) of photo in b.

5. Discussion

As previously discussed, the basic approach of this study was mainly focused on finding field and ore microscopy elements that are able to: (1) unravel the reciprocal relationships between ore deposit types and (2) provide indications on the controls operated by the Variscan tectonic structures during mineralization events in the Baccu Locci mine area.

Previous works have usually considered the occurrence of *type a* sulphide lenses in the Baccu Locci mine area as a single ore. This was interpreted in different ways, essentially trying to establish genetic links with different phases of mineralization and with the *type b* ores. Thus, according to a proposed “syndimentary” model, the Zn–Cu–Pb sulphides would represent an initial (predeformation) concentration of metals (*proto-ore*) that, remobilized during Variscan deformation, provided the sulphide component to *type b* veins [37,40]. An interesting issue was first raised by the study of Zucchetti [38], which evidenced a partial superposition of mineral assemblages in both ores. This was considered as indicative of an origin of Zn–Cu–Pb sulphides by lateral infilling from Qtz–As–Pb sulphide veins, but without clearly distinguishing the two mineralization in space and time.

Structural data and ore mineralogy observations that were carried out with this study document a complex mineralization history, including two distinct kinds of polyphasic ores (here, *type a* and *type b* ores in this text) that show different minerals assemblage and different spatial relationships with tectonic structures (Figure 13).

	1	2			3
STRUCTURAL REGIME	<i>Passive infilling of sulphides in D1 mylonite foliation occurred after D2 Variscan phase</i>	<ul style="list-style-type: none"> • D4 strike-slip tectonics. Development of large dilational jogs in NW-SE dextral strike-slip (reverse movement) faults. • Reopening of foliation in hinge zone of antiforms. • Mafic diking. • Repeated cataclasis of ores, including type-a and early type-b 			<i>Late cataclasis of ores</i>
MINERALIZING EVENT	<i>Zn-Cu ORE STAGE: Lenticular sulphide orebodies (TYPE-A ORE)</i>	<i>Pre-ORE STAGE: Swarms of NW-SE high-angle Qtz veins also crosscutting type-a ores</i>	<i>As-Fe ORE STAGE: infilling of quartz and arsenopyrite in cataclased pre-ore quartz veins (TYPE-B ORE) and in cataclased type-a ore</i>	<i>Pb-Zn-Cu-(Sb, Au) ORE STAGE: diffuse infilling of sulphides in cataclased TYPE-A and TYPE-B ores and in mafic dikes.</i>	<i>Post-ORE STAGE: swarms of barren veinlets crosscutting all previous orebodies</i>
Quartz	—————	—————	—————	—————	—————
Scheelite		- - - - - ?	- - - - - ?		
Arsenopyrite			—————	—————	
Pyrite			—————	—————	—————
Galena				—————	
Chalcopyrite	—————			—————	
Sphalerite	—————			—————	
Pyrrhotite	—————				
Tetrahedrite				—————	
Gold-Electrum			- - - - - ?	- - - - - ?	

Figure 13. Evolution of mineralizing events in the Baccu Locci mine area and their relationships with tectonic events.

5.1. Relationships between Ore Type Deposits

The *type a* ore crops out in the Spilloncargiu mine, where the Zn–Cu sulphide lenses are cut by a swarm of *type b* veins (Figure 14). Ore microscopy evidence corroborates the relationships at the outcrop scale; in fact, *type a* minerals (mainly sphalerite, calcopyrite, and pyrrhotite) are strongly cataclased and *type b* minerals (mainly galena and chalcopyrite with subordinate arsenopyrite and tetrahedrite) infill the voids that were created by cataclasis. These textures confirm that *type b* postdates *type a* mineralization and that a brittle tectonic event occurred in between. In turn, the *type b* minerals

show mutual crosscutting relationships that demonstrate the progressive and polyphased deposition of white quartz (pre-ore stage in Figure 13), arsenopyrite (As–Fe stage), and galena (Pb–Zn–Cu–Sb–Au stage) as the most abundant mineral phases. This *type b* mineral assemblage is well represented in the San Riccardo/Su Spinosu ore, where the ore paragenesis is not associated with a *type a* ore and linkage between the ore and transpressive dextral faults is manifest. Furthermore, ore microscopy shows that between the several *type b* mineralizing stages, there are progressive mutual relationships of cataclasis and successive mineral infilling, showing that *type b* was synkinematic with a brittle deformation. The post-ore stage of mineralization (cryptocrystalline quartz, pyrite) is widespread and crosscuts all of the previous mineral assemblages, so it postdates the main mineralizing events. Only in *type b* veins does gold occurrence assume economic relevance. On the contrary, a lack of significant gold grades in *type a* mineralization is noteworthy; it could be related to lower content in arsenopyrite, which has been recorded in other areas of the Gerrei–Sarrabus district as a probable first carrier for gold (Brecca mine: [5,41]).

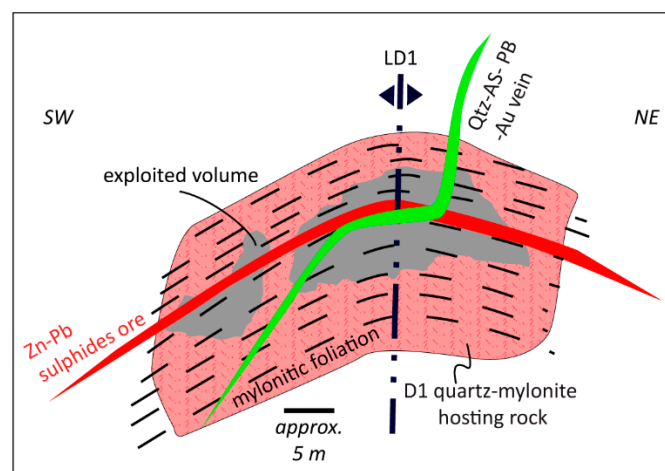


Figure 14. Sketch of the mutual relationships between *type a* and *type b* ores located at the top of LD1 antiform hinge zone.

5.2. Orebody/Tectonic Structure Relationships and Structural Control

The *type a* ore is hosted in the mylonites that characterize the Baccu Locci shear zone and it is located at the top of the hinge of a large LD1 antiform that folded together bedding, D1 folding axial-plane foliation, and mylonitic foliation. Interpreting the mylonite as Silurian black shales, some previous studies considered the tectonic foliation as primary bedding and classified the ores as stratiform and synsedimentary of probable volcano-exhalative origin [37,40]. From the definition of the Baccu Locci mylonitic shear zone [3], it is well established that the Zn–Cu sulphide lenses developed parallel to D1 Variscan foliations, in both the axial plane and mylonitic (Figure 6a). Furthermore, *type a* Zn–Cu sulphides show no physical relationship with the Ordovician metavolcanics (“Porfiroidi” Fm., Figures 3 and 5) that crop out as less deformed tectonic slices in the Baccu Locci shear zone. On the whole, these geometric relationships clearly rule out the possible syngenetic (“stratiform” or “stratabound”) options for mineralization, excluding any connection between the primary bedding (now completely obliterated by the Variscan tectonic imprint) and orebodies. Similarly, field relationships and ore textures exclude possible syn-D1 (“syn-metamorphic”) deposition; in fact, the sulphides infill the D1 foliations but they are not in turn affected by them. In this way, the LD1 hinge zone operated as a typical structural trap, but it essentially exerted “passive” structural control, because there is no evidence of synkinematic formation of mineral deposits. At the Gerrei–Sarrabus district scale, *type a* ores have not been recognized in places other than hinge zones of LD1 folds, also by the extensive surveys that were made during mine exploitation. Further confirmation may be found in an adjacent LD1 antiform, a few kilometers west of the study area (Riu Gruppa

antiform, Sa Lilla mine; Figure 2), where previously reputed “stratoid” orebodies of sulphides, similar by mineral association and texture [42] to those of Baccu Locci/Spilloncargiu, are located at the top of a comparable hinge zone, in which development of sulphide “beds” was once again parallel to the D1 tectonic foliations.

Some speculation can be made about the modality that allowed the brittle reactivation of horizontal tectonic foliations to create space for *type a* mineral deposition. Structural data point out that *type a* ores postdate D1 and LD1 structures. Further, the creation of horizontal lens-shaped voids now filled with mineral deposits during the D2 extensional phase sounds unrealistic, because the vertical stress σ_1 (that we can image roughly higher than the lithostatic stress) operating during the rocks’ exhumation would have prevented the opening of subhorizontal discontinuities. So, we can argue that *type a* ores could have been developed after the Gerrei and Rio Gruppa tectonic units got to shallower crustal levels, where the fluid pressure could overcome the lithostatic stress, possibly when the vertical stress σ_1 related to the extensional dynamics ceased. The role of decreased lithostatic stress in allowing for the development of open spaces that are suitable for mineralization should be confirmed by the absence of similar orebodies in deeper parts of the hinge zone. Anyway, this interpretation can be demonstrated when data about the baric environment are available. Up to now, the only available data from fluid inclusions [10] highlight that a metamorphic environment can be excluded, thus mineralization might postdate D2 deformation.

The *type b* Qtz–As–Pb veins are hosted in narrow brittle–ductile shear zones, generally developed inside the quartz–mylonitic rocks. We described their occurrence in the Spilloncargiu mine at the top of an LD1 antiform, where they cut at low angle *type a* ore, but they reach their main thickness in the San Riccardo/Su Spinosu mine. There, the availability of detailed mineworks plans permitted the recognition of the tectonic relationship and highlighted the occurrence of large dilational jogs (Figure 13). Interestingly, there are close relationships between jog geometry and older D1–LD1–D2 structures, although jogs clearly postdate them. In fact, the San Riccardo main fault is a generally WSW–steepening dipping transpressive fault that mostly cuts at high angle the NE-dipping D1 foliation in the northeast limb of LD1 antiform (Figure 15). The fault abruptly changes the dip direction to WSW, gently dipping just where it crosses gently SW-dipping D1 foliation in the reverse limb of a D2 recumbent fold (Figure 15). So, dilational jogs developed when the D4 fault reactivated preexisting anisotropies (in this case, D1 tectonic foliations) if they had the right attitude. Ore mineralogy shows repeated cataclasis and mineral infilling during the several mineralizing stages of *type b* veins, suggesting a progressive brittle deformation that in some cases produced large dilational jogs that were suitable to host orebodies with economic relevance [43,44]. Actually, the most important mineral assemblage—the galena- (and gold-) rich ore related to the Pb–Zn–Cu–Sb–Au stage of mineralization (Figure 13)—is associated with the largest jogs. The jog structures are not perfectly cylindrical, so their geometries can change slightly along strikes (Figure 11). This is probably due to a change in the D1 foliation attitude in the reverse limbs of D2 recumbent folds or to a change of the local stress field.

The recognition of such large dilational jogs is not very common [44] and it has been possible by the availability of observations at different scales. Moreover, the case of Baccu Locci/San Riccardo reveals that the occurrence of previous reactivable foliation, possibly with different attitude due to a polyphase deformation, can be one of the situations suitable for the development of large jogs. In the study area, the understanding of such active structural control would allow a different way to find new, possibly more fruitful, orebodies. In the case study, the change in dip direction of D1 tectonic foliation on the limbs of LD1 folds could be ignored, because it is not directly linkable with the mineralized veins, but it could be a clue to identify the occurrence of large dilational jogs.

Finally, some considerations might be given to the relationships between mafic dikes and the Qtz–As–Pb sulphide vein system, which is problematic. The definition of possible genetic links between the mafic magmatism and the mineralization processes falls well outside the scope of this work, requiring a wider geochemical study at the district scale. However, field mapping and explorations into the old mineworks showed several mutual relationships between dikes and ore veins (Figure 12).

These spatial relationships suggest a coeval emplacement. Mafic dikes may have intruded in an interval between the main mineralizing events of *type b* ore, in particular, between the first and second mineralization stages (pre-ore/As–Fe sulphide stages) and the third stage (sulphide/sulfosalts stage) of the paragenetic sequence, producing apparently contrasting timing relationships in the field. Under this hypothesis, considering the age available for these rocks in the neighboring areas [13], mafic dikes assume a chronological constraint, suggesting an age of mineralizing events around 302 Ma; that is, an age in which the Variscan basement of southern Europe suffered a widespread tectonic extension. This age is, in fact, consistent with: (a) ^{40}Ar – ^{39}Ar dating of hydrothermal white mica in quartz–arsenopyrite–gold veins in the nearby Monte Ollasteddu area (307 ± 3 Ma) [10], and (b) several geological constraints occurring in the whole Gerrei district [26], indicating that the quartz–arsenopyrite–gold vein systems clearly predate the previously described mineralized vein systems related to F-bearing granites, dated at 286 Ma [9,12], and they are unconformably covered by lower Permian sediments dated at 295 Ma [13]. However, it cannot be excluded that the latest stages of mineralization in Baccu Locci (including the *type b* Pb–Zn–Cu–Sb–Au sulphide/sulfosalts stage that affects the mafic dikes) could be related to events referable to the younger part of the outlined chronological interval. Overall, these constraints allow for us to consider the ore deposits of the Baccu Locci mine area as part of a much wider metallogenic event that affected various massifs of the Variscan orogen between 310 and 300 Ma [45,46]. From their geological, mineralogical, and geochemical characteristics, they can be best classified as Variscan orogenic gold type [47]. As in other massifs of European Variscides, in Sardinia this metallogenic event involved a crustal-scale flow of fluids during the late Variscan extension, resulting in widespread mineralizing processes in major regional structures, such as the Flumendosa Antiform. Large shear zones, such as the Baccu Locci shear zone, are part of the main plumbing system through which deep fluids were focused toward the shallower parts of the crust.

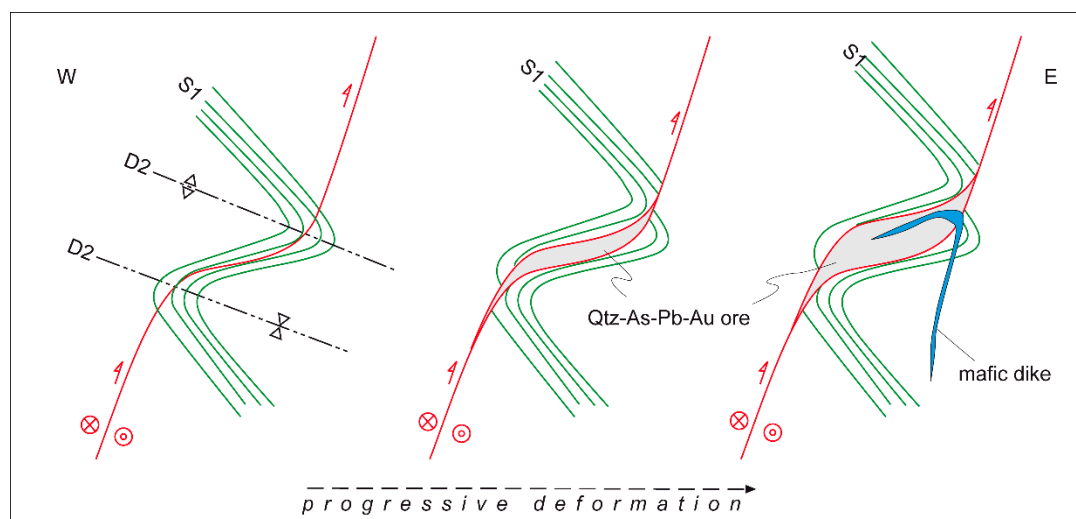


Figure 15. Baccu Locci/San Riccardo mine: scheme of the geometric relationships between foliation, faults, mafic dikes, and Qtz–As–Pb sulphide veins. See the location of this structure in the larger LD1 antiform in the cross-section in Figures 3 and 4.

6. Conclusions

The ores in Baccu Locci are a good example of structurally controlled mineralization in a basement characterized by the overprinting of several tectonic phases, from ductile to brittle, during both compressive and extensional regimes. The control exerted was either a passive reactivation of older foliations to create space for mineral deposition, or an active syn-kinematic deposition of minerals during the progressive evolution of the hosting structure. In particular, the emplacement of the older types of ores exposed in Baccu Locci emerges as the result of the opening of previous discontinuities

(foliations) in the hinge zone of large antiforms, where they are subhorizontal, after their exhumation to shallow structural levels when postcollisional extension ceased. Afterward, a different stress field produced transpressive faults that reactivated anisotropic surfaces parallel to the axial plane in the hinge zone. Along the transpressive dextral faults, large dilational jogs developed, whose geometry was influenced by sudden changes of the attitude of Variscan foliation in the reverse limbs of recumbent folds. The jogs formed together with mineral deposits, exerting in this way an “active” control of mineralization and hosting the more economically relevant ores. As a general statement, the occurrence of older tectonic foliations and folds might be taken into account not only because they can be directly presumed to be hosting mineralized veins, a common concept in the study of structure–orebody relationships, but also when considering the influence that they could have in modifying hosting structures and favoring the formation of more significant orebodies, being in this way a good tool for prospecting new relevant ores.

Although the overprinting relationships between the different ores and the mafic dikes are now clearer, more data are needed to better constrain the thermobaric environment in which the minerals were deposited, the time interval between them, the source of the ore fluids, and finally the role of mafic dikes in the large frame of the Late Variscan metallogenic epoch in Sardinia.

Author Contributions: A.F., A.D., and S.N. conceptualized the study. A.F. performed the geological mapping. A.F., C.B., and F.C. performed the structural analysis and 3D structural modelling. A.D. and S.N. performed the orebodies' survey. S.N. performed the macro to micro-scale ore mineralogy. A.F. and S.N. wrote the original draft and with C.B. and F.C. reviewed and edited the draft. Funding acquisition and project administration were performed by A.F. and S.N.

Funding: This research was funded by FdS-RAS Fondazione di Sardegna and Regione Autonoma della Sardegna grant number F72F16003080002 and by Italian Government, project PRIN-2005 grant number 2005047008.

Acknowledgments: The authors are grateful to two anonymous reviewers for their comments that improved the quality of the paper and thank the editors for the careful editorial management.

Conflicts of Interest: The authors declare no conflict of interest.

References

- Conti, P.; Carmignani, L.; Oggiano, G.; Funedda, A.; Eltrudis, A. From thickening to extension in the Variscan belt—Kinematic evidence from Sardinia (Italy). *Terra Nova* **1999**, *11*, 93–99. [CrossRef]
- Funedda, A.; Naitza, S.; Conti, P.; Dini, A.; Buttau, C.; Tocco, S.; Carmignani, L. The geological and metallogenic map of the Baccu Locci mine area (Sardinia, Italy). *J. Maps* **2011**, *2011*, 103–114. [CrossRef]
- Conti, P.; Funedda, A.; Cerbai, N. Mylonite development in the Hercynian basement of Sardinia (Italy). *J. Struct. Geol.* **1998**, *20*, 121–133. [CrossRef]
- Funedda, A.; Naitza, S.; Conti, P.; Dini, A.; Buttau, C.; Tocco, S.; Carmignani, L. Structural control of ore deposits: The Baccu Locci shear zone (SE Sardinia). *Rend. Online SGI* **2011**, *15*, 66–68.
- Lerouge, C.; Bouchot, V.; Douguet, M.; Naitza, S.; Tocco, S.; Funedda, A. *Variscan Gold Mineralisation of Baccu Locci and Brecca, Southeastern Sardinia: Petrographic and Geochemical Studies*; BRGM Report N RP-54431-FR; BRGM: Orleans, France, 2007; p. 47. Available online: <http://infoterre.brgm.fr/rapports/RP-54431-FR.pdf> (accessed on 13 October 2018).
- Conti, P.; Carmignani, L.; Funedda, A. Change of nappe transport direction during the Variscan collisional evolution of central-southern Sardinia (Italy). *Tectonophysics* **2001**, *332*, 255–273. [CrossRef]
- Cocco, F.; Funedda, A. The Sardinic Phase: Field evidence of Ordovician tectonics in SE Sardinia, Italy. *Geol. Mag.* **2017**, *1–14*. [CrossRef]
- Carmignani, L.; Conti, P.; Barca, S.; Cerbai, N.; Eltrudis, A.; Funedda, A.; Oggiano, G.; Patta, E.D.; Ulzega, A.; Orrù, P.; et al. *Foglio 549-Muravera. Note Illustrative*; Servizio Geologico d'Italia: Roma, Italy, 2001; p. 140.
- Conte, A.M.; Cuccuru, S.; D'Antonio, M.; Naitza, S.; Oggiano, G.; Secchi, F.; Casini, L.; Cifelli, F. The post-collisional late Variscan ferroan granites of southern Sardinia (Italy): Inferences for inhomogeneity of lower crust. *Lithos* **2017**, *294–295*, 263–282. [CrossRef]

10. Dini, A.; Di Vincenzo, G.; Ruggieri, G.; Rayner, J.; Lattanzi, P. Monte Ollasteddu, a new late orogenic gold discovery in the Variscan basement of Sardinia (Italy)—Preliminary isotopic (^{40}Ar - ^{39}Ar , Pb) and fluid inclusion data. *Miner. Depos.* **2005**, *40*, 337–346. [[CrossRef](#)]
11. Cortesogno, L.; Cassinis, G.; Dallagiovanna, G.; Gaggero, L.; Oggiano, G.; Ronchi, A.; Seno, S.; Vanossi, M. The Variscan post-collisional volcanism in Late Carboniferous-Permian sequences of Ligurian Alps, Southern Alps and Sardinia (Italy): A synthesis. *Lithos* **1998**, *45*, 305–328. [[CrossRef](#)]
12. Ronca, S.; Del Moro, A.; Traversa, G. Geochronology, Sr-Nd isotope geochemistry and petrology of Late Hercynian dike magmatism from Sarrabus (SE Sardinia). *Period. Mineral.* **1999**, *68*, 231–260.
13. Dack, A. Internal Structure And geochronology of the Gerrei Unit in the Flumendosa Area, Variscan External Nappe Zone, Sardinia, Italy. Master's Thesis, Boise State University, Boise, ID, USA, 2009.
14. Cassinis, G.; Ronchi, A. Upper Carboniferous to Lower Permian continental deposits in Sardinia (Italy). *Geodiversitas* **1997**, *19*, 217–220.
15. Carmignani, L.; Carosi, R.; Di Pisa, A.; Gattiglio, M.; Musumeci, G.; Oggiano, G.; Pertusati, P.C. The Hercynian chain in Sardinia (Italy). *Geodin. Acta* **1994**, *7*, 31–47. [[CrossRef](#)]
16. Conti, P.; Patta, E.D. Large scale W-directed tectonics in southeastern Sardinia. *Geodin. Acta* **1998**, *11*, 217–231. [[CrossRef](#)]
17. Carosi, R.; Musumeci, G.; Pertusati, P.C. Senso di trasporto delle unità tettoniche erciniche della Sardegna dedotto dagli indicatori cinematici nei livelli cataclastico-milonitici. *Rend. Soc. Geol. Ital.* **1990**, *13*, 103–106.
18. Casini, L.; Funedda, A. Potential of pressure solution for strain localization in the Bacchu Locci Shear Zone (Sardinia, Italy). *J. Struct. Geol.* **2014**, *66*, 188–204. [[CrossRef](#)]
19. Casini, L.; Funedda, A.; Oggiano, G. A balanced foreland-hinterland deformation model for the Southern Variscan belt of Sardinia, Italy. *Geol. J.* **2010**, *45*, 634–649. [[CrossRef](#)]
20. Funedda, A. Foreland- and hinterland-verging structures in fold-and-thrust belt: An example from the Variscan foreland of Sardinia. *Int. J. Earth Sci.* **2009**, *98*, 1625–1642. [[CrossRef](#)]
21. Funedda, A.; Meloni, M.A.; Loi, A. Geology of the Variscan basement of the Laconi-Asuni area (central Sardinia, Italy): The core of a regional antiform refolding a tectonic nappe stack. *J. Maps* **2015**, *11*, 146–156. [[CrossRef](#)]
22. Montomoli, C.; Iaccarino, S.; Simonetti, M.; Lezzerini, M.; Carosi, R. Structural setting, kinematics and metamorphism in a km-scale shear zone in the Inner Nappes of Sardinia (Italy). *Ital. J. Geosci.* **2018**, *137*, 294–310. [[CrossRef](#)]
23. Carmignani, L.; Pertusati, P.C. Analisi strutturale di un segmento della catena ercinica: Il Gerrei (Sardegna sud-orientale). *Boll. Soc. Geol. Ital.* **1977**, *96*, 339–364.
24. Carmignani, L.; Oggiano, G.; Barca, S.; Conti, P.; Salvadori, I.; Eltrudis, A.; Funedda, A.; Pasci, S. *Geologia della Sardegna. Note Illustrative della Carta Geologica in Scala 1:200.000*; Servizio Geologico d'Italia: Roma, Italy, 2001.
25. Carmignani, L.; Cortecchi, G.; Dessau, G.; Duchi, G.; Oggiano, G.; Pertusati, P.; Saitta, M. The antimony and tungsten deposit of Villasalto in South-Eastern Sardinia and its relationship with Hercynian tectonics. *Schweiz. Mineral. Petrogr. Mitt.* **1978**, *58*, 163–188.
26. Funedda, A.; Naitza, S.; Tocco, S. Caratteri giacimentologici e controlli strutturali nelle mineralizzazioni idrotermali tardo-erciniche ad As-Sb-W-Au del basamento metamorfico paleozoico della Sardegna Sud-orientale. *Resoconti dell'Associazione Mineraria Sarda* **2005**, *110*, 25–46.
27. Garbarino, C.; Naitza, S.; Tocco, S.; Farci, A.; Rayner, J. Orogenic Gold in the Paleozoic Basement of SE Sardinia. In *Mineral Exploration an Sustainable Development*; Eliopoulos, D.G., Ed.; Mill Press: Rotterdam, The Netherlands, 2003; pp. 767–770.
28. Naitza, S.; Oggiano, G.; Cuccuru, S.; Casini, L.; Puccini, A.; Secchi, F.; Funedda, A.; Tocco, S. Structural and magmatic controls on Late Variscan Metallogenesis: Evidences from Southern Sardinia (Italy). In *Mineral Resources in a Sustainable World, Proceedings of the 13th Biennial SGA Meeting, Nancy, France, 24–27 August 2015*; André-Mayer, A.S., Cathelineau, M., Muchez, P.H., Pirard, E., Sindern, S., Eds.; The Society for Geology Applied to Mineral Deposits (SGA): Nancy, France, 2015; pp. 161–164.
29. Naitza, S.; Conte, A.M.; Cuccuru, S.; Oggiano, G.; Secchi, F.; Tecce, F. A Late Variscan tin province associated to the ilmenite-series granites of the Sardinian Batholith (Italy): The Sn and Mo mineralisation around the Monte Linas ferroan granite. *Ore Geol. Rev.* **2017**, *80*, 1259–1278. [[CrossRef](#)]

30. Belkin, H.E.; De Vivo, B.; Valera, R. Fluid inclusion study of some Sarrabus fluorite deposits, Sardinia, Italy. *Econ. Geol.* **1984**, *79*, 409–414. [[CrossRef](#)]
31. Boni, M.; Balassone, G.; Fedele, L.; Mondillo, N. Post-Variscan hydrothermal activity and ore deposits in southern Sardinia (Italy): Selected examples from Gerrei (Silius Vein System) and the Iglesias district. *Period. Mineral.* **2009**, *78*, 19–35.
32. Giamello, M.; Protano, G.; Riccobono, F.; Sabatini, G. The W-Mo deposit of Perda Majori (SE Sardinia, Italy): A fluid inclusion study of ore and gangue minerals. *Eur. J. Mineral.* **1992**, *4*, 1079–1084. [[CrossRef](#)]
33. Allmendinger, R.W.; Cardozo, N.; Fisher, D. *Structural Geology Algorithms: Vectors and Tensors*; Cambridge University Press: Cambridge, UK, 2012; p. 302.
34. Lena, G.; Barchi, M.R.; Alvarez, W.; Felici, F.; Minelli, G. Mesosstructural analysis of S-C fabrics in a shallow shear zone of the Umbria–Marche Apennines (Central Italy). *Geol. Soc. Lond. Spec. Publ.* **2018**, *409*, 149–166. [[CrossRef](#)]
35. Rutter, E.H.; Maddock, R.H.; Hall, S.H.; White, S.H. Comparative microstructures of natural and experimentally produced clay-bearing fault gouges. *Pure Appl. Geophys.* **1986**, *124*, 3–30. [[CrossRef](#)]
36. Barton, P.B.; Bethke, P.M. Chalcopyrite disease in sphalerite: Pathology and epidemiology. *Am. Mineral.* **1987**, *72*, 451–467.
37. Bakos, F.; Carcangiu, G.; Fadda, S.; Mazzella, A.; Valera, R. The gold mineralization of Baccu Locci (Sardinia, Italy): Origin, evolution and concentration processes. *Terra Nova* **1990**, *2*, 232–237. [[CrossRef](#)]
38. Zucchetti, S. The lead-arsenic-sulfide ore deposit of Bacu Locci (Sardinia-Italy). *Econ. Geol.* **1958**, *53*, 867–876. [[CrossRef](#)]
39. Hancock, P.L. Brittle microtectonics: Principles and practice. *J. Struct. Geol.* **1985**, *7*, 437–457. [[CrossRef](#)]
40. Schneider, H.-J. Schichtgebundene NE-Metall- und F-Ba-Lagerstätten im Sarrabus-Gerrei-Gebiet, SE-Sardinien. I. Bericht: Zur Lagerstättenkunde und Geologie. *Neues Jahrb. Mineral. Monatshefte* **1972**, 529–541.
41. Lerouge, C.; Naitza, S.; Bouchot, V.; Funedda, A.; Tocco, S. Invisible gold in arsenopyrite of the Variscan Au-Sb Brecca mineralization (Gerrei district, Southeastern Sardinia). *Geol. Fr.* **2007**, *2*, 124.
42. Violo, M. Contributo alla conoscenza dei giacimenti stratoidi polimetallici, in area metamorfica. Il giacimento di Sa Lilla (San Vito, Cagliari-Sardegna). *Resoconti dell'Associazione Mineraria Sarda* **1966**, *71*, 5–110.
43. Cox, S.F.; Braun, J.; Knackstedt, M.A. Principles of structural control on permeability and fluid flow in hydrothermal systems. *Rev. Econ. Geol.* **2001**, *14*, 1–24.
44. Robert, F.; Poulsen, K.H. Vein formation and deformation in greenstone gold deposits. *Rev. Econ. Geol.* **2001**, *14*, 111–155.
45. Bouchot, V.; Ledru, P.; Lerouge, C.; Lescuyer, J.L.; Milesi, J.P. Late Variscan mineralizing systems related to orogenic processes: The French Massif Central. *Ore Geol. Rev.* **2005**, *27*, 169–197. [[CrossRef](#)]
46. De Boorder, H. Spatial and temporal distribution of the orogenic gold deposits in the Late Palaeozoic Variscides and Southern Tianshan: How orogenic are they? *Ore Geol. Rev.* **2012**, *46*, 1–31. [[CrossRef](#)]
47. Bouchot, V.; Milesi, J.P.; Ledru, P. Crustal Scale Hydrothermal Palaeofield and Related Au, Sb, W Orogenic Deposits at 310–305 Ma (French Massif Central, Variscan Belt). *SGA News* **2000**, *10*, 6–12.

